Received: 20 September 2021 | Revised: 6 January 2022 | Accepted: 10 January 2022

DOI: 10.1002/mrm.29179

TECHNICAL NOTE

Magnetic Resonance in Medicine

Whole-brain mapping of mouse CSF flow via HEAP-METRIC phase-contrast MRI

Juchen Li[1,2] | **Mengchao Pei**[2] | **Binshi Bo**[2] | **Xinxin Zhao**[4] | **Jing Cang**[1] | **Fang Fang**[1] | **Zhifeng Liang**[2,3]

[1]Department of Anesthesia, Zhongshan Hospital, Fudan University, Shanghai, People's Republic of China

[2]Institute of Neuroscience, CAS Key Laboratory of Primate Neurobiology, Center for Excellence in Brain Science and Intelligence Technology, Chinese Academy of Sciences, Shanghai, People's Republic of China

[3]Shanghai Center for Brain Science and Brain-Inspired Intelligence Technology, Shanghai, People's Republic of China

[4]Department of Radiology, Shanghai Cancer Institute, Ren Ji Hospital, School of Medicine, Shanghai Jiao Tong University, Shanghai, People's Republic of China

Correspondence
Zhifeng Liang, Institute of Neuroscience, CAS Key Laboratory of Primate Neurobiology, Center for Excellence in Brain Science and Intelligence Technology, Chinese Academy of Sciences, Shanghai 200031, China.
Email: zliang@ion.ac.cn

Funding information
Supported by the Chinese Academy of Sciences (CAS) Strategic Priority Research Program, grant (XDB32030100); the Shanghai Municipal Science and Technology Major Project, grant (2018SHZDZX05); the National Natural Science Foundation of China (NSFC), grant (81771821); and the CAS Pioneer Hundred Talents Program, and Clinical Research Project of Shanghai Health Committee, grant (20194Y0087)

Purpose: CSF plays important roles in clearing brain waste and homeostasis. However, mapping whole-brain CSF flow in the rodents is difficult, primarily due to its assumed very low velocity. Therefore, we aimed to develop a novel phase-contrast MRI method to map whole-brain CSF flow in the mouse brain.

Methods: A novel generalized Hadamard encoding–based multi-band scheme (dubbed HEAP-METRIC, Hadamard Encoding APproach of Multi-band Excitation for short TR Imaging aCcelerating) using complex Hadamard matrix was developed and incorporated into conventional phase contrast (PC)-MRI to significantly increase SNR.

Results: Slow flow phantom imaging validated HEAP-METRIC PC-MRI's ability to achieve fast and accurate mapping of slow flow velocities (~10^2 μm/s). With the SNR gain afforded by HEAP-METRIC scheme, high-resolution (0.08 × 0.08 mm in-plane resolution and 36 0.4 mm slices) PC-MRI was completed in 21 min for whole-brain CSF flow mapping in the mouse. Using this novel method, we provide the first report of whole-brain CSF flow in the awake mouse brain with an average flow velocity of ~200 μm/s. Furthermore, HEAP-METRIC PC-MRI revealed CSF flow was reduced by isoflurane anesthesia, accompanied by reduction of glymphatic function as measured by dynamic contrast-enhanced MRI.

Conclusion: We developed and validated a generalized HEAP-METRIC PC-MRI for mapping low velocity flow. With this method, we have achieved the first whole-brain mapping of awake mouse CSF flow and have further revealed that anesthesia reduces CSF flow velocity.

Juchen Li and Mengchao Pei contributed equally to this work.

KEYWORDS
cerebrospinal fluid, Hadamard encoding, low velocity flow, mouse CSF flow, multi-band excitation, phase-contrast MRI

1 | INTRODUCTION

Recently, CSF has been increasingly recognized for its role in brain waste clearance and homeostasis. Produced by choroid plexus, CSF flows from the ventricular system into the subarachnoid space and exits via the cranial and spinal nerves and arachnoid granulations.[1] The glymphatic theory[2–4] suggests an expanded role of CSF because it enters brain parenchyma through paravascular space and exchanges with interstitial fluid.

CSF flow is believed to be driven mostly by arterial pulsation[5] but is also influenced by respiration[6,7] and lower frequency components such as vasomotion.[8] CSF flow has been found to be related to cognitive deficits in aging[9,10] and levels of certain proteins,[11] suggesting its important role.

However, CSF flow mapping in rodents is difficult because invasive methods are likely to alter it, whereas noninvasive methods such as conventional phase contrast (PC)-MRI can only map CSF flow in humans (or large animals) where it is relatively fast (on the order of ~10^4 μm/s[12,13]). Because rodents have much smaller brains, their CSF flow is likely several orders of magnitude slower than humans. This poses a challenge for PC-MRI for 2 reasons: First, low SNR maps are heavily contaminated by Rician noise, and thus velocity images have large bias errors.[14–16] Second, slow flow velocities require high amplitude toggling gradients in PC-MRI, leading to phase errors caused by high eddy current field.[17–19]

Therefore, we aimed to develop a novel PC-MRI method capable of mapping slow flows, such as mouse CSF flow. A novel generalized Hadamard encoding–based multi-band (HEAP-METRIC) scheme was developed for substantially increased SNR with high multi-band factors in PC-MRI.

2 | METHODS

2.1 | HEAP-METRIC PC-MRI

A multi-band excitation RF waveform is expressed as the sum of individual RF pulses with different on-resonance frequencies:

$$W(t) = A(t) \cdot \sum_{m=1}^{N} e^{i\omega_m t}, \tag{1}$$

where $W(t)$ denotes a time-dependent multi-band RF waveform; $A(t)$ denotes a standard single-band selective excitation pulse waveform (e.g., a sinc or hyperbolic secant); N is number of simultaneous bands (or slices); m is the band index; and ω_m is the on-resonance frequency of m^{th} band. With Hadamard-encoding phase modulation, a set of N RF waveforms is generated (Figure 1), and Equation (1) becomes:

$$W_n(t) = A(t) \cdot \sum_{m=1}^{N} e^{i(\omega_m t + \varphi_{nm})}, \tag{2}$$

where n denotes the HEAP-METRIC RF pulse index; φ_{nm} denotes the Hadamard encoding phase of m^{th} band of n^{th} RF waveform. With elements $e^{i\varphi_{nm}}$, an $N \times N$ Hadamard matrix is constructed:

$$H = \left\{ e^{i\varphi_{nm}} \right\} = \begin{bmatrix} e^{i\varphi_{11}} \cdots e^{i\varphi_{1N}} \\ \vdots \quad \ddots \quad \vdots \\ e^{i\varphi_{N1}} \cdots e^{i\varphi_{NN}} \end{bmatrix} \quad n, m \in [1, N]. \tag{3}$$

$\boldsymbol{H}$ is orthogonal and satisfies Equation (4):

$$HH^* = NI, \tag{4}$$

where $\boldsymbol{I}$ is the identity matrix; $\boldsymbol{H}^*$ is the conjugate transpose of $\boldsymbol{H}$. Previous work[20–24] utilized real Hadamard matrices with ±1 entries (equivalent to $\varphi_{nm} = 0^{\text{o}}$ or 180^{o}); thus, N is limited to 2 or $4k$ (k is an integer). Here, the Hadamard matrix is complex; thus, N can be any arbitrary integer. Fourier basis vectors are used to construct our new Hadamard matrix $H = \left\{ e^{i\frac{nm2\pi}{N}} \right\}$.

The MR signal excited by the n^{th} HEAP-METRIC RF pulse is then formulated as:

$$S_n = \sum_{m=1}^{N} X_m \cdot e^{i\varphi_{nm}}, \tag{5}$$

which is simplified as Equation (6):

$$S = HX. \tag{6}$$

Because $\boldsymbol{H}$ is orthogonal, each individual band signal $\boldsymbol{X_m}$ is obtained by Equation (7):

$$X_m = \sum_{n=1}^{N} S_n \cdot e^{-i\varphi_{nm}}, \tag{7}$$

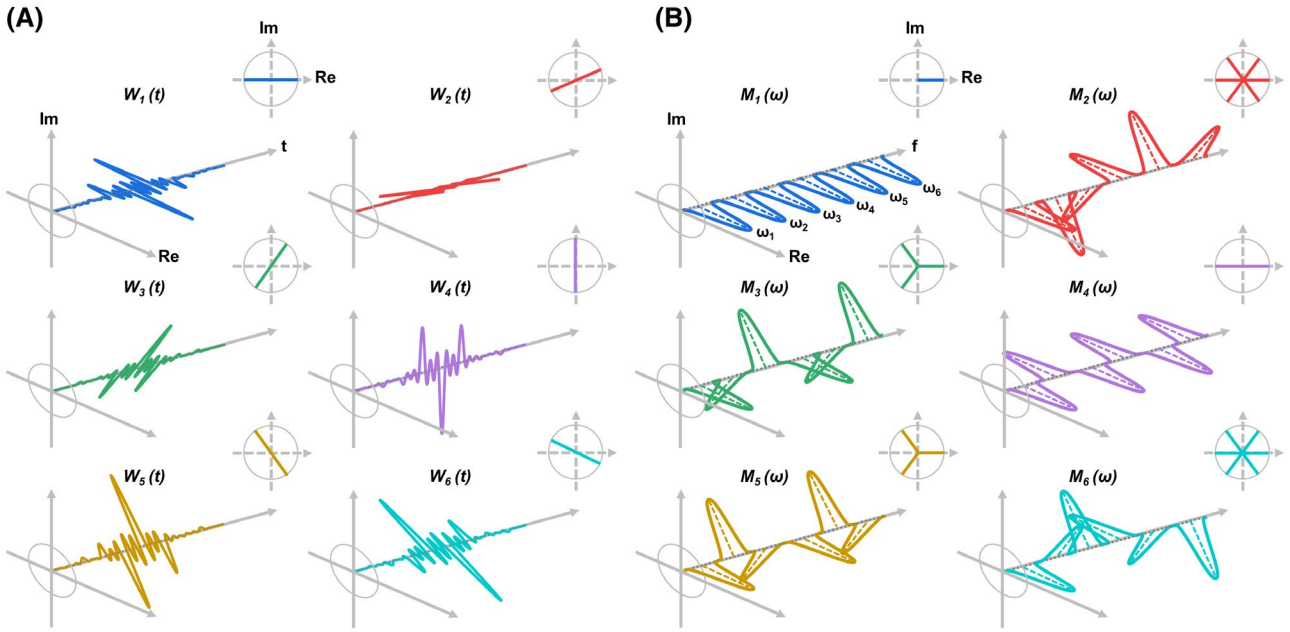

FIGURE 1 HEAP-METRIC RF waveform design and excitation profiles. (A) HEAP-METRIC RF waveforms using MB factor 6 as an example ($W_1(t)$-$W_6(t)$). Each waveform was plotted as a time-dependent 3D complex pulse with a projection on complex plane at its upper right corner. In actual experiments, an MB factor 18 was used. (B) Excitation profiles $M_1(\omega)$-$M_6(\omega)$ of $W_1(t)$-$W_6(t)$ as calculated by Bloch equations. Each profile was plotted as a frequency-dependent 3D complex curve with a projection on a complex plane at its upper right corner. Each band of each profile is rotated on the complex plane by a certain phase angle according to the Hadamard matrix. HEAP-METRIC, Hadamard Encoding APproach of Multi-band Excitation for short TR Imaging aCcelerating

which again is simplified as Equation (8)

$$X = H^* S. \tag{8}$$

N separated scans are required to obtain all N bands images. Comparing with single-band approaches, HEAP-METRIC provides N times signal averages with N simultaneous slices with identical acquisition time. Therefore, HEAP-METRIC increases SNR per time by a factor of $\sqrt{N}$.

The aforementioned HEAP-METRIC scheme was incorporated into conventional PC-MRI (Figure 2A). A group of HEAP-METRIC 18-band RF waveforms were designed. All excited bands of HEAP-METRIC pulses were designed to be equally spaced. Adjacent bands were gapped by 1 band distance; thus, it required 2 slice selections to complete a whole brain scan. Images were reconstructed using Equation (8) (Figure 2B) with 36 slices in total. Its looping structure is listed in Supporting Information Figure S1.

To cancel eddy current effects, we postprocessed phase contrast images by spatial polynomial regression on static tissues. Results were then subtracted by estimated eddy field[17–19,25] (Figure 2C). The above procedures were done separately on data of 3 velocity-encoding directions (read, phase, and slice). Three directional velocity maps were combined as in Equation (9) to generate velocity magnitude maps (Figure 2D).

$$V_{mag} = \sqrt{V_{read}^2 + V_{phase}^2 + V_{slice}^2}, \tag{9}$$

where V_{mag}, V_{read}, V_{phase}, and V_{slice} denote velocity magnitude; velocities of readout; phase encoding; and slice components, respectively.

2.2 | Phantom HEAP-METRIC PC-MRI experiment

All imaging experiments were conducted on a Bruker 9.4 Tesla scanner, with the HEAP-METRIC pulse sequence implemented in Bruker ParaVision 6.0.1.

For phantom experiments, a silicone tubing and a 10 ml syringe were connected into a fluid flow system using a syringe pump (Harvard Apparatus) (Figure 3A). Artificial CSF fluid was pumped in the silicone tubing, which was placed into a holder filled with 1% agarose. Flow rates were set to average velocities of 100, 200, 300, 400, 500, and 600 μm/s, in this order, with a minimum of a 5-min gap between switching flow rates, to allow stable flow. Imaging parameters were TR/TE 30/9.1 ms, flip angle 10º, receiver bandwidth 100 kHz, FOV 16 × 16 mm^2, matrix size 180 × 200, slice thickness 0.4 mm, and VENC value 1500 μm/s.

2.3 | Animal HEAP-METRIC PC-MRI experiment

Male adult C57BL/6 mice were used ($N = 6$ for anesthetized imaging and $N = 7$ for awake imaging) with food and water

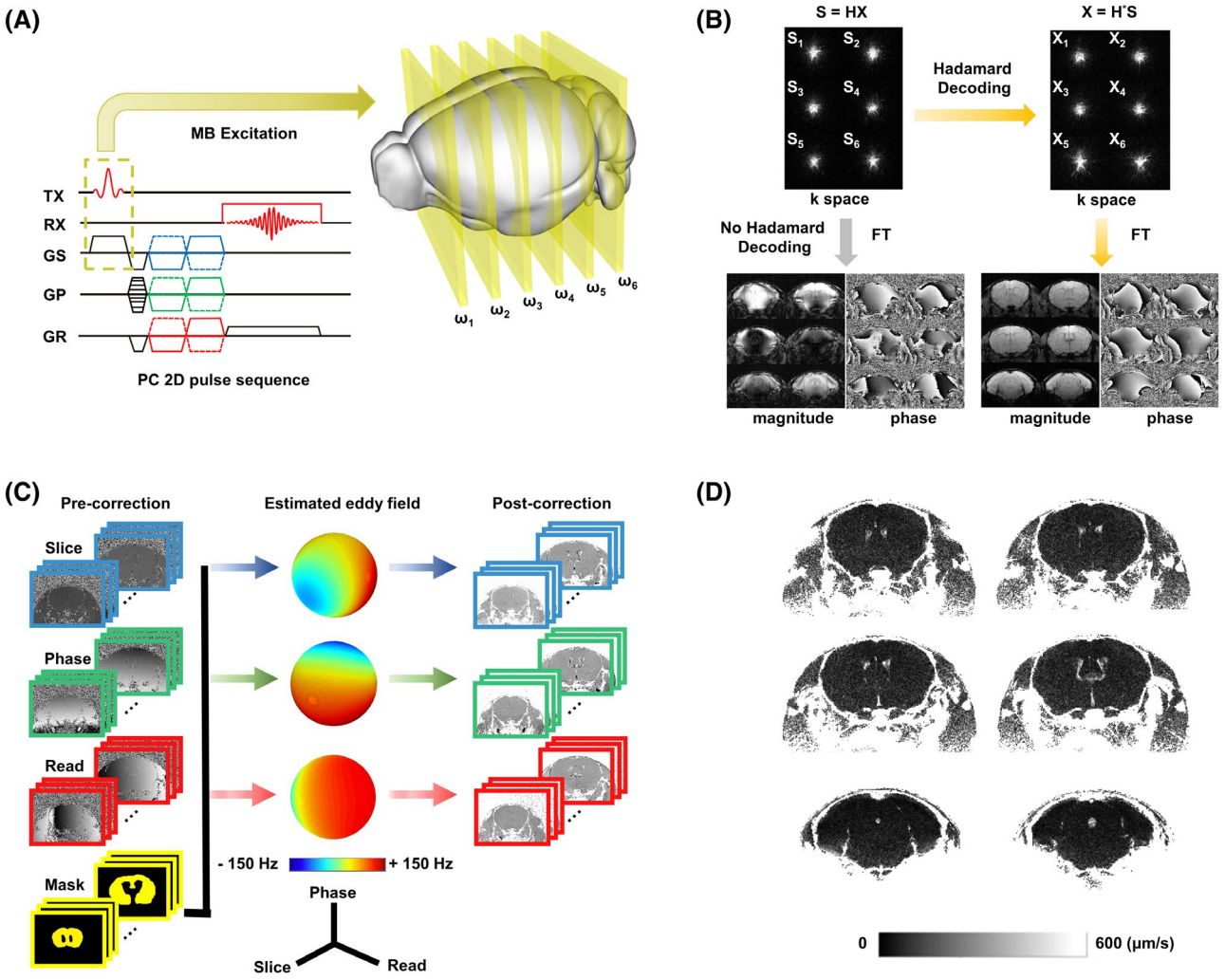

FIGURE 2 HEAP-METRIC PC-MRI for mouse CSF velocity mapping. (A) Illustration of 6-band HEAP-METRIC RF pulses applied on a PC 2D sequence for mouse CSF velocity mapping. (B) Reconstruction of HEAP-METRIC data. The k-space data were Hadamard decoded and Fourier transformed to obtain magnitude and phase images. Images reconstructed without Hadamard decoding are displayed in lower left as a comparison but were not used. (C) Eddy current field shimming. Left column: raw phase contrast images of 3 velocity encoding directions (slice, phase, and read) and manually drawn masks on static tissues. Middle column: 3 spherical maps of eddy current fields estimated by second-order spatial polynomial fitting on the static field. Right column: phase images after phase correction including unwrapping and shimming. (D) Final quantitative CSF velocity magnitude maps after combination of 3 directional results. PC, phase contrast

ad libitum. All animal experiments were approved by Animal Care and Use Committee of Institute of Neuroscience, Chinese Academy of Sciences, Shanghai, China.

For awake imaging, awake mouse preparation and imaging setup were done according to our previous studies.[26,27] Briefly, a head holder was implanted above the animal's skull for head fixation. After recovery from the implantation surgery, mice were acclimated to the MRI environment with head fixation and recorded imaging noises.

For anesthetized imaging group, mice were initially anesthetized with 5% isoflurane and intubated. During imaging, mice were mechanically ventilated at 80 breaths per min using 1.3% isoflurane delivered by mixed oxygen and air (20%: 80%). Rectal temperature was monitored and maintained at 37 ± 0.5°C, and respiratory and cardiac signals were also recorded (SA Instruments, Inc).

Imaging parameters were TR/TE 30/9.1 ms, flip angle 10°, receiver bandwidth 100 kHz, FOV 16 × 16 mm^2, matrix size 200 × 200, slice thickness 0.4 mm, VENC value 1500 μm/s. Total scanning time was 21.8 min.

2.4 | Animal DCE-MRI experiment

Dynamic contrast-enhanced MRI was utilized to assess the glymphatic function in awake ($N = 6$) and isoflurane-anesthetized ($N = 5$) conditions. Animal preparation and

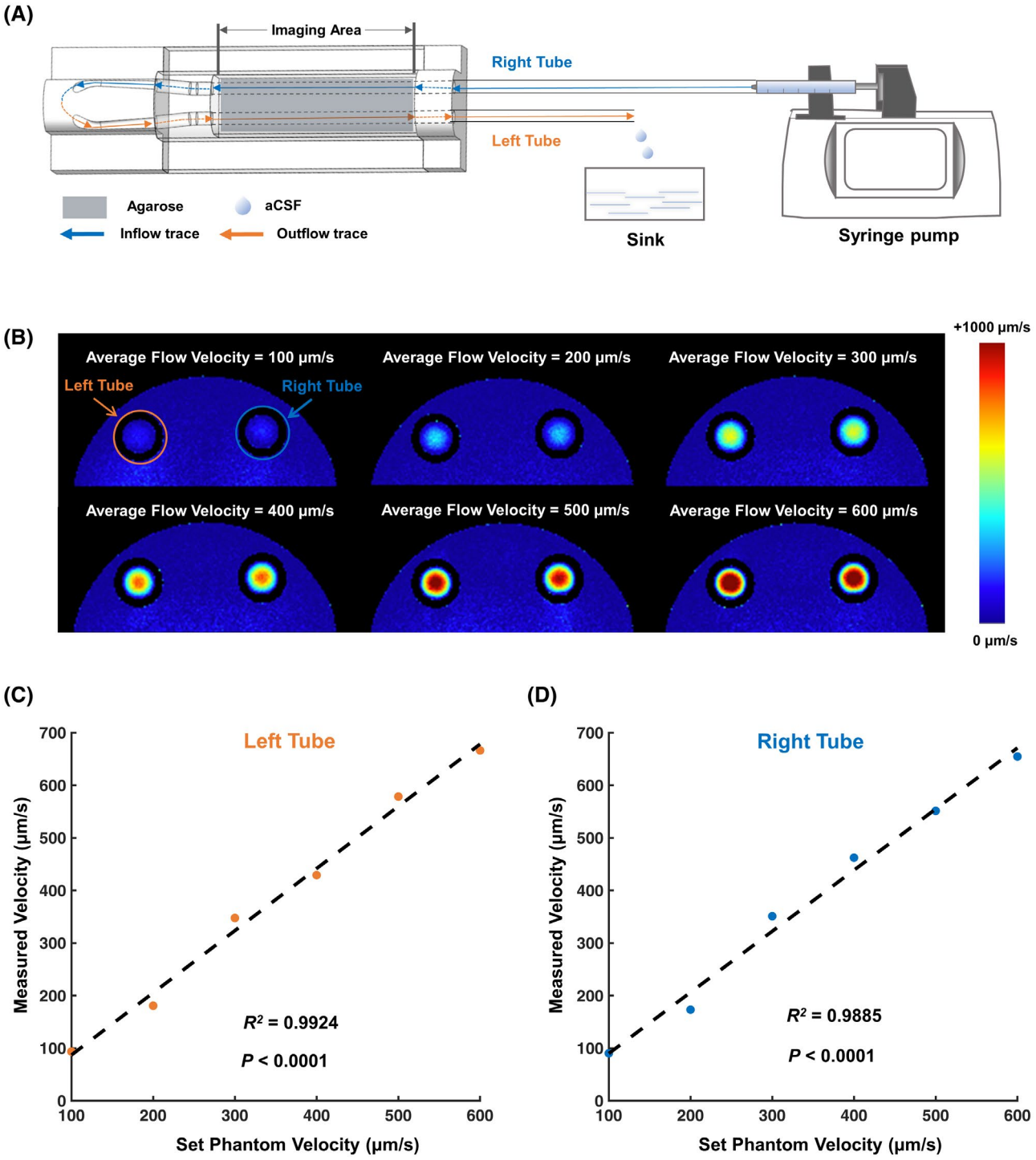

FIGURE 3 Phantom experiment validates HEAP-METRIC PC-MRI velocity mapping. (A) Diagram of slow flow phantom. (B) HEAP-METRIC velocity magnitude mapping of flow phantom with set averaged flow velocity from 100–600 µm/s. (C,D) High correlation between the measured velocity magnitude and the set phantom velocity in the left ($R^2 = 0.9924$, $P < .0001$) and right tube ($R^2 = 0.9885$, $P < .0001$), respectively

imaging setup were done according to previous studies.[28,29] Standard stereotaxic surgery was conducted to insert a custom-made glass capillary (tip diameter 100–150 µm) into the cisterna magna as previously described.[30] Awake and anesthetized imaging setups were the same as described in the above session.

T_1-weighted 3D-FLASH images were continuously acquired every 4 min. The contrast agent (Gd-DTPA: aCSF = 1:40) was infused at a rate of 0.8 µl/min for a total volume of 10 µl at the beginning of the fourth scan. Forty scans were acquired continuously for 160 min for each animal.

2.5 | Data analysis

All data were processed using custom scripts in MatLab (MathWorks, Natick, MA), SPM12 (http://www.fil.ion.ucl.ac.uk/spm/), and ITK-SNAP (http://www.itksnap.org/).

First, MR images were normalized to the mouse brain template (https://www.nitrc.org/projects/tpm_mouse) using nonlinear symmetric normalization algorithm in ANTs. CSF mask generation has been summarized in Supporting Information Figure S2. Specifically, a tissue probabilistic atlas (including gray matter, white matter, CSF, tissues outside the brain, and air) was used as a spatial prior for anatomical MRI image segmentation. Then, the CSF mask (marked red in Supporting information Figure S2) was created by thresholding the segmented CSF probability map with probability > 0.9. Finally, minor manual correction was applied to remove nonventricle regions to generate the final CSF mask.

The final CSF mask was applied in the corresponding velocity image to calculate the mean CSF velocity. The Allen mouse atlas (https://atlas.brain-map.org/) was utilized to further extract different ventricles (lateral ventricle, third ventricle, fourth ventricle, and cerebral aqueduct) (Supporting Information Figure S3). The above ventricle-specific masks were used to obtain mean CSF velocity of each ventricle.

For dynamic contrast-enhanced MRI data, all images were corrected for head motion and spatially smoothed. The percentage of signal changes from the baseline (before Gd-DTPA infusion) were calculated in each voxel as previously described[12] and then were averaged to obtain the whole brain signal.

3 | RESULTS

In the current work, HEAP-METRIC, a generalized Hadamard encoding scheme using complex Hadamard matrix, was developed as described in Methods. Figures 1 and 2 illustrate the HEAP-METRIC RF waveform design and HEAP-METRIC PC-MRI for mouse CSF velocity mapping, respectively.

HEAP-METRIC PC-MRI was validated using a slow flow phantom because the mapping results showed high correlation with set average flow velocities ranging from 100–600 μm/s when using magnitude (Figure 3) or phase contrast (slice component) (Supporting Information Figure S4) velocity results (summarized in Supporting Information Table S1). Furthermore, HEAP-METRIC acquisition with MB factors showed highly similar results with single slice acquisition with a matched number of averages (Supporting Information Figure S5). Therefore, HEAP-METRIC PC-MRI clearly demonstrated the capability of multi-slice low velocity flow mapping.

The substantial SNR gain from the HEAP-METRIC scheme is critical because low SNR PC-MRI suffered from a large bias error in both in vivo CSF (Figure 4) and phantom mapping (Supporting Information Figure S6). Higher MB factors (and thus higher SNR) enabled by the HEAP-METRIC scheme resulted in increasingly smaller bias error in velocity magnitude maps (Figure 4 and S6) and a reduction of signal variations (Supporting Information Figure S5).

Using our novel method, and in combination with our previously established awake mouse MRI method,[26,27] we characterized ventricular CSF flow at the whole brain level in awake mice. MB factor of 18 was used to achieve high resolution (0.08 × 0.08 mm in plane resolution) and whole brain (36 0.4 mm slices) CSF mapping (Figure 5) in 21.8 min. In contrast, conventional single band acquisition would require 388.8 min (and thus be infeasible in vivo). Whole-brain CSF flowed at very low velocity (average velocity 216.89 μm/s) (Figure 5D) in the awake condition and exhibited spatial heterogeneity (Figure 5A, D). As expected, CSF flowed at higher speeds within narrow spaces, such as cerebral aqueduct, compared to within the much larger lateral ventricles (Figure 5A, D). In addition to the velocity, we observed a clear directional CSF flow in various structures, including the lateral ventricles, third ventricle, and cerebral aqueduct (Supporting Information Figure S7), which is within general agreement with the current understanding of CSF circulation. For example, the direction of CSF flow in the lateral ventricle was mainly dorsal–ventral, whereas the direction was mainly anteroposterior in the third ventricle and cerebral aqueduct (slice direction).

Importantly, HEAP-METRIC PC-MRI revealed significant reduction of CSF velocity under isoflurane anesthesia (Figure 5B, D), which has not been reported before. Such reduction was not spatially uniform because it was more pronounced in third and fourth ventricles. When pooled with awake data, we found significant correlation between heart rate and averaged CSF velocity (Supporting Information Figure S8), suggesting a possible physiological basis for anesthesia-induced CSF velocity reduction. Interestingly, the same isoflurane anesthesia was found to reduce the glymphatic function (as measured by dynamic contrast-enhanced MRI) compared to the awake condition (Supporting Information Figure S9), suggesting a potential link between macroscopic ventricular CSF flow and microscopic CSF-ISF flow in brain parenchyma.

4 | DISCUSSION

We developed HEAP-METRIC PC-MRI to allow noninvasive and whole brain mapping of low-velocity CSF flow

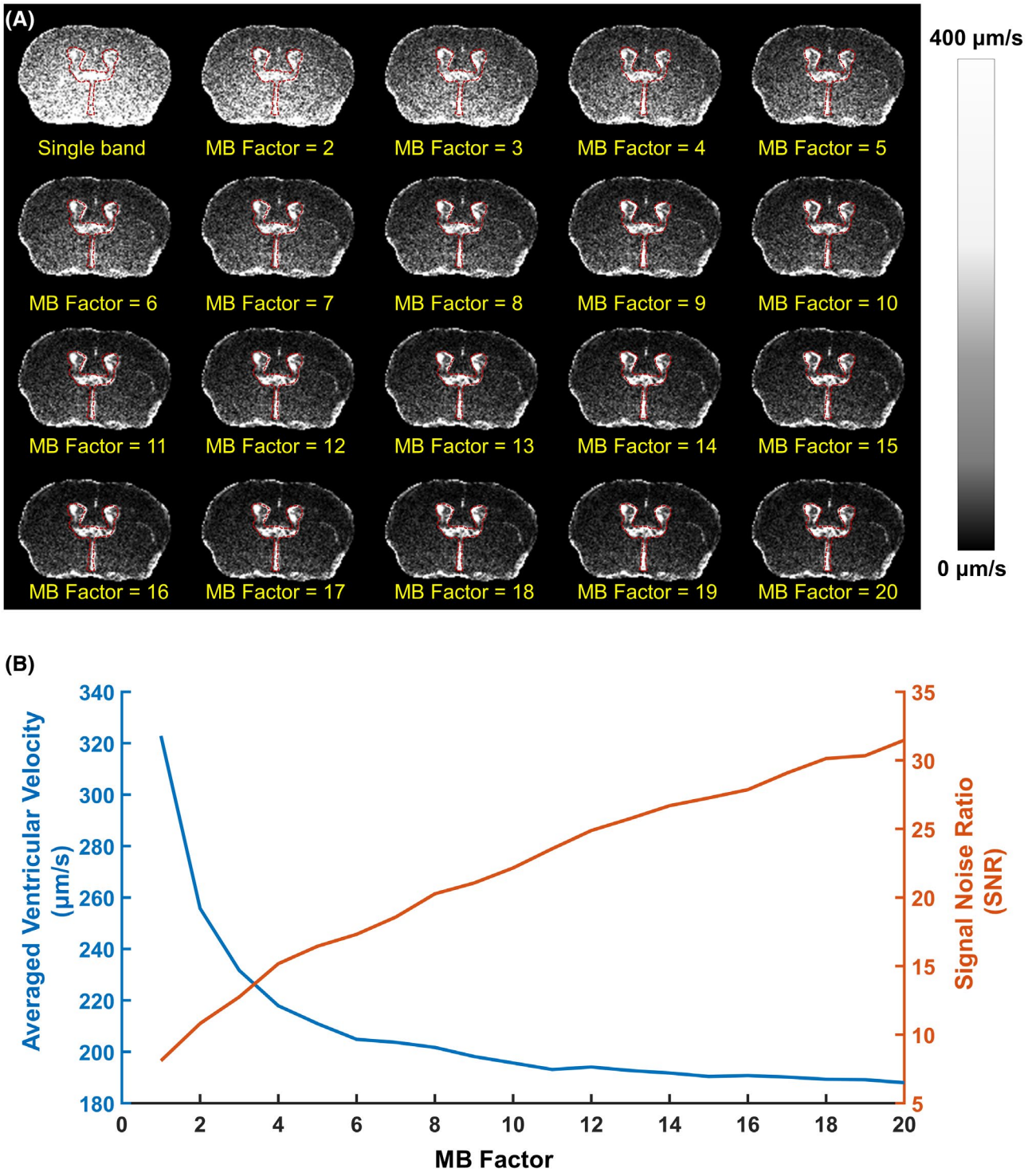

FIGURE 4 Reduction of bias errors in velocity mapping with SNR improvement with the HEAP-METRIC scheme. (A) Reconstructed quantitative velocity magnitude maps from conventional single-band imaging versus MB factors from 2–20 showed notable reduction of bias errors with increasing MB factors. Red outlines are manually drawn CSF ventricle ROIs. (B) Averaged ventricular velocity and SNR (based on ventricular ROI in (A)) exhibited decreasing and increasing trends, respectively, with increasing MB factors. ROI, region of interest

in the mouse brain. We found directional and regionally heterogeneous CSF flow at a whole-brain average velocity of 216 μm/s in awake mice. Furthermore, compared to the awake state, isoflurane anesthesia reduced whole-brain average velocity to 182 μm/s. This reduction was correlated with heart rate decrease and accompanied by reduction of glymphatic function.

The major obstacle to mapping CSF flow in mouse was that when velocity magnitude maps were recorded with low SNR, they would be heavily contaminated by

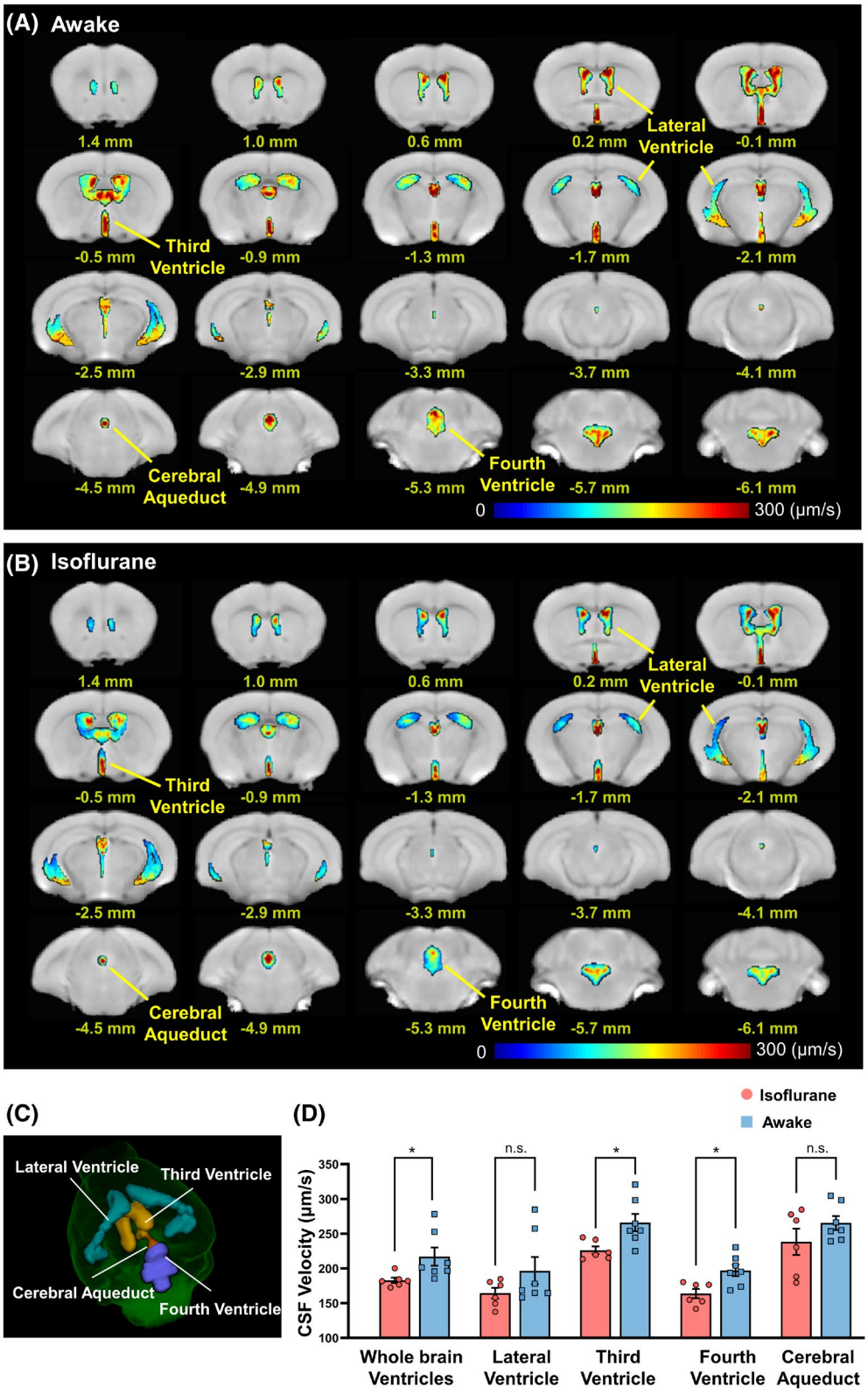

FIGURE 5 Whole brain mapping of mouse ventricular CSF flow in awake condition and its reduction by isoflurane anesthesia. (A,B) cerebral ventricular CSF velocity mapping in the awake (A, $n = 6$) and isoflurane anesthesia (B, $n = 7$) conditions. Numbers under each slice denote the relative distance from bregma. (C) Illustration of 3D reconstructed cerebral ventricle definition. (D) Reduction of CSF flow by isoflurane anesthesia at the whole brain and individual ventricle levels. *, $P < .05$. Whole brain ventricles: $P = .04$, third ventricle: $P = .02$, fourth ventricle: $P = .01$

Rician noise, which creates large bias errors in velocity images.[14–16] To increase PC-MRI's SNR gained versus time spent, we developed HEAP-METRIC scheme to achieve simultaneous multi-slice imaging. For N slice acquisition, this scheme achieves N averages and thus an SNR increase of $\sqrt{N}$, which proved critical for mapping slow CSF flow in the mouse brain.

Previous Hadamard MB encoding methods required the MB factor to be 2 or $4k$ (k is an integer), which is mathematically required for a real Hadamard matrix. The current HEAP-METRIC approach uses a complex orthogonal matrix to achieve a general form of Hadamard encoding, taking advantage of the fact that the MR signal is complex. Thus, any arbitrary number of slices for Hadamard encoding acquisition can be achieved. This new HEAP-METRIC scheme can be extended to other short TR MRI applications, including TOF sequences for vascular imaging, FLASH, or SSFP sequences for multi-slice cardiac imaging, as well as EPI sequences for fMRI, to boost SNR versus time.

Because mice are a key animal model used in neuroscience research, our novel method paves the way for dissecting roles of genetic, physiological, or pathological factors that affect CSF flow. To the best of our knowledge, the current study is the first whole-brain characterization of CSF flow velocity and its direction in the mouse brain. The high spatial resolution and whole-brain coverage allowed us to perform a detailed and unbiased examination of CSF flow in the ventricular system, for example, the aqueduct. The aqueduct is a small but important structure in the ventricular system that connects the third and fourth ventricles. At its narrowest point, the cross-sectional dimension is 0.25×0.1 mm (width $\times$ height) and at the widest point is 0.72×0.5 mm. The high spatial resolution, enabled by the high SNR of our HEAP-METRIC scheme, was sufficient to measure the flow in the aqueduct (Figure 5) (Supporting Information Figure S7). However, higher spatial resolution in the future might still be beneficial to reduce the partial volume effect at its narrowest point (~3 voxels).

It is known that CSF flow is pulsatile and dependent on cerebral arterial pulsation,[5] respiration,[6,7] and lower frequency components including vasomotion.[8] In the current study, we revealed that isoflurane anesthesia reduced CSF flow velocity compared to the awake condition. The detailed mechanism underlying this reduction may be complex and requires further study. However, the correlation between heart rate and CSF velocity that we observed (Supporting Information Figure S8) indicates it might be related to the reduction of cerebral arterial pulsation under anesthesia.

Interestingly, we also observed a reduction of glymphatic function under anesthesia (Supporting Information Figure S9). One major component of the glymphatic system is the CSF–ISF exchange in brain parenchyma, and evidence shows that cerebral arterial pulsation drives this exchange.[31] Therefore, arterial pulsation may be the common driver for both ventricular CSF flow and CSF-ISF exchange. Thus, the decreased heart rate (Supporting Information Figure S8) might be the common factor behind the reduction in both CSF flow and glymphatic function under isoflurane anesthesia. It is also possible that there is direct relationship between the CSF flow and glymphatic function, which requires further investigation.

The current study was limited by a few factors: First, the HEAP-METRIC scheme is unable to speed up single slice imaging or acquisition without signal averaging (NEX =1) but instead provides increased SNR in multi-slice short TR acquisitions. Although such SNR increase per time is critical for mapping mouse CSF flow velocity (Figure 4), the current whole-brain mapping protocol still takes ~20 min. Second, due to this relatively long acquisition time, cardiac or respiratory gated flow mapping was not achieved in the current study. Thus, the current CSF flow mapping is a time-averaged net flow. However, CSF flow is known to be pulsatile.[5] Therefore, understanding its exact temporal dynamics will require substantial improvement on the current method to achieve cardiac or respiratory gated CSF flow mapping. Furthermore, head motion and physiological variation during the ~20 min acquisition may have affected the mapping quality. Although our awake mouse setup[26,27] was optimized for minimizing head motion, understanding the impact of physiological (e.g., cardiac) fluctuations will require further study. Lastly, whereas the current VENC value of 1500 μm/s is within a reasonable range with a maximum CSF velocity around 700 μm/s, it is also constrained by our gradient strength because lower values require longer TEs, which leads to SNR loss and higher risks of susceptibility artifact-induced phase errors.

5 | CONCLUSION

In conclusion, we developed HEAP-METRIC PC-MRI for whole-brain mapping of mouse CSF flow velocity. Furthermore, we revealed that isoflurane anesthesia reduced both CSF flow velocity and glymphatic function compared to the awake condition. The HEAP-METRIC scheme can be further extended to other MR techniques to boost SNR versus time.

ACKNOWLEDGEMENT

This work was supported by the Chinese Academy of Sciences (CAS) Strategic Priority Research Program (XDB32030100), Shanghai Municipal Science and Technology Major Project (2018SHZDZX05), NSFC

(81771821), CAS Pioneer Hundred Talents Program, and Clinical Research Project of Shanghai Health Committee (20194Y0087). The authors thank Garth J. Thompson from ShanghaiTech University for helpful comments.

DATA AVAILABILITY STATEMENT

The HEAP-METRIC sequence is made openly available (https://github.com/ZhifengLiangLab/HEAP-METRIC.git).

ORCID

Zhifeng Liang https://orcid.org/0000-0003-2758-1194

REFERENCES

1. Shapey J, Toma A, Saeed SR. Physiology of cerebrospinal fluid circulation. *Curr Opin Otolaryngol Head Neck Surg*. 2019;27:326-333.
2. Plog BA, Nedergaard M. The glymphatic system in central nervous system health and disease: past, present, and future. *Annu Rev Pathol*. 2018;13:379-394.
3. Nedergaard M, Goldman SA. Glymphatic failure as a final common pathway to dementia. *Science*. 2020;370:50-56.
4. Rasmussen MK, Mestre H, Nedergaard M. The glymphatic pathway in neurological disorders. *Lancet Neurol*. 2018;17:1016-1024.
5. Preuss M, Hoffmann K-T, Reiss-Zimmermann M, et al. Updated physiology and pathophysiology of CSF circulation—the pulsatile vector theory. *Childs Nerv Syst*. 2013;29:1811-1825.
6. Dreha-Kulaczewski S, Joseph AA, Merboldt KD, Ludwig HC, Gärtner J, Frahm J. Identification of the upward movement of human CSF in vivo and its relation to the brain venous system. *J Neurosci*. 2017;37:2395-2402.
7. Dreha-Kulaczewski S, Joseph AA, Merboldt KD, Ludwig HC, Gärtner J, Frahm J. Inspiration is the major regulator of human CSF flow. *J Neurosci*. 2015;35:2485-2491.
8. van Veluw SJ, Hou SS, Calvo-Rodriguez M, et al. Vasomotion as a driving force for paravascular clearance in the awake mouse brain. *Neuron*. 2020;105:549-561.e5.
9. Stoquart-ElSankari S, Balédent O, Gondry-Jouet C, Makki M, Godefroy O, Meyer ME. Aging effects on cerebral blood and cerebrospinal fluid flows. *J Cereb Blood Flow Metab*. 2007;27:1563-1572.
10. Attier-Zmudka J, Sérot J-M, Valluy J, et al. Decreased cerebrospinal fluid flow is associated with cognitive deficit in elderly patients. *Front Aging Neurosci*. 2019;11:87.
11. Puy V, Zmudka-Attier J, Capel C, et al. Interactions between flow oscillations and biochemical parameters in the cerebrospinal fluid. *Front Aging Neurosci*. 2016;8:154.
12. Sakhare AR, Barisano G, Pa J. Assessing test-retest reliability of phase contrast MRI for measuring cerebrospinal fluid and cerebral blood flow dynamics. *Magn Reson Med*. 2019;82:658-670.
13. Tawfik AM, Elsorogy L, Abdelghaffar R, Naby AA, Elmenshawi I. Phase-contrast MRI CSF flow measurements for the diagnosis of normal-pressure hydrocephalus: observer agreement of velocity versus volume parameters. *Am J Roentgenol*. 2017;208:838-843.
14. Gudbjartsson H, Patz S. The Rician distribution of noisy MRI data. *Magn Reson Med*. 1995;34:910-914.
15. Andersen AH, Kirsch JE. Analysis of noise in phase contrast MR imaging. *Med Phys*. 1996;23:857-869.
16. Constantinides CD, Atalar E, McVeigh ER. Signal-to-noise measurements in magnitude images from NMR phased arrays. *Magn Reson Med*. 1997;38:852-857.
17. Callaghan FM, Burkhardt B, Geiger J, Valsangiacomo Buechel ER, Kellenberger CJ. Flow quantification dependency on background phase correction techniques in 4D-flow MRI. *Magn Reson Med*. 2020;83:2264-2275.
18. Espe EK, Zhang L, Sjaastad I. Unwrapping eddy current compensation: improved compensation of eddy current induced baseline shifts in high-resolution phase-contrast MRI at 9.4 Tesla. *Magn Reson Med*. 2014;72:1096-1102.
19. Lorenz R, Bock J, Snyder J, Korvink JG, Jung BA, Markl M. Influence of eddy current, Maxwell and gradient field corrections on 3D flow visualization of 3D CINE PC-MRI data. *Magn Reson Med*. 2014;72:33-40.
20. Müller S. Multifrequency selective RF pulses for multislice MR imaging. *Magn Reson Med*. 1988;6:364-371.
21. Souza SP, Szumowski J, Dumoulin CL, Plewes DP, Glover G. SIMA: simultaneous multislice acquisition of MR images by Hadamard-encoded excitation. *J Comput Assist Tomogr*. 1988;12:1026-1030.
22. Goelman G. Fast 3D T(2)-weighted MRI with Hadamard encoding in the slice select direction. *Magn Reson Imaging*. 2000;18:939-945.
23. Saritas EU, Lee D, Çukur T, Shankaranarayanan A, Nishimura DG. Hadamard slice encoding for reduced-FOV diffusion-weighted imaging. *Magn Reson Med*. 2014;72:1277-1290.
24. Goelman G, Liu S, Gonen O. Reducing voxel bleed in Hadamard-encoded MRI and MRS. *Magn Reson Med*. 2006;55:1460-1465.
25. Lankhaar JW, Hofman MB, Marcus JT, Zwanenburg JJ, Faes TJ, Vonk-Noordegraaf A. Correction of phase offset errors in main pulmonary artery flow quantification. *J Magn Reson Imaging*. 2005;22:73-79.
26. Han Z, Chen W, Chen X, et al. Awake and behaving mouse fMRI during Go/No-Go task. *NeuroImage*. 2019;188:733-742.
27. Chen X, Tong C, Han Z, et al. Sensory evoked fMRI paradigms in awake mice. *NeuroImage*. 2020;204:116242.
28. Mestre H, Du T, Sweeney AM, et al. Cerebrospinal fluid influx drives acute ischemic tissue swelling. *Science*. 2020;367:eaax7171.
29. Benveniste H, Lee H, Ding F, et al. Anesthesia with dexmedetomidine and low-dose isoflurane increases solute transport via the glymphatic pathway in rat brain when compared with high-dose isoflurane. *Anesthesiology*. 2017;127:976-988.
30. Xavier ALR, Hauglund NL, von Holstein-Rathlou S, et al. Cannula implantation into the cisterna magna of rodents. *J Vis Exp*. 2018;135:57378.
31. Iliff JJ, Wang M, Zeppenfeld DM, et al. Cerebral arterial pulsation drives paravascular CSF-interstitial fluid exchange in the murine brain. *J Neurosci*. 2013;33:18190-18199.

SUPPORTING INFORMATION

Additional supporting information may be found in the online version of the article at the publisher's website.

FIGURE S1 Looping structure of HEAP-METRIC PC-MRI pulse sequence

FIGURE S2 Flowchart of CSF mask generation

FIGURE S3 Atlas-based cerebral ventricular definition
FIGURE S4 Same as in Figure 3 in the main text, but using phase contrast (slice component) information
FIGURE S5 HEAP-METRIC method (MB factors 2-20) was highly similar to single slice acquisition with averages (NEX 1-20) in flow phantom velocity measurements
FIGURE S6 Reduction of bias errors in velocity magnitude mapping with SNR improvement in the phantom flow mapping at the set averaged velocity of 200 μm/s
FIGURE S7 Representative CSF flow directions revealed by HEAP-METRIC mapping
FIGURE S8 Heart rate was correlated with whole-brain CSF velocity
FIGURE S9 Isoflurane anesthesia reduced the glymphatic function compared to the awake condition using DCE-MRI
Table S1 Set and measured velocities in the phantom experiment

How to cite this article: Li J, Pei M, Bo B, et al. Whole-brain mapping of mouse CSF flow via HEAP-METRIC phase-contrast MRI. *Magn Reson Med*. 2022;87:2851–2861. doi:10.1002/mrm.29179